Chapter 3

Regulating Adult Human Mesenchymal Stem Cells (hMSCs) Response Through Bioengineered Platforms

3.1 Introduction

Titanium is a commonly used biomaterial supporting cell proliferation and differentiation process [161-163]. Extensive work has been done on surface modification of titanium to enhance its properties for inducing differentiation of mesenchymal stem cells into the osteogenic lineage [164, 165]. However, limited work has been focused on exploring titanium oxide coating for transforming hMSCs into non-endodermal origin, including neuronal lineage. The platforms discussed in chapter 2 were engineered to modify the intrinsic characteristics of TiO_2 coating with a dopant of variable electronegativity that may be conducive to neurogenic differentiation of stem cells.

The *in-vitro* cytotoxicity assessment of the coated platforms was assessed using a calorimetric method, MTT (3-[4,5-dimethylthiozol-2yl]-2,5-diphenyl tetrazolium bromide) assay [166] as well as fluorescence-based technique, Hoechst 33342/PI dual staining [167]. Further, to confirm the introduction of dopant in titanium oxide surfaces promote the neurogenic differentiation of mesenchymal stem cells *in-vitro*, different neural-specific markers, nestin, β-tubulin III, and glial fibrillary acidic protein (GFAP) were quantified by immunocytochemistry. Nestin, a neuro-ectodermal stem cell marker, is a type VI intermediate filament protein that is predominantly expressed by neural stem cells [168]. The neural stem cells are progenitor cells that can differentiate into committed neural sub-types, neurons, astrocytes, and oligodendrocytes expressing β tubulin-III, GFAP, and O4 markers, respectively [169]. To find out the cellular processes for modulating neurodifferentiation of hMSCs, change in intracellular reactive oxygen species (ROS) level was investigated. Earlier

studies suggest that excessive oxidative stress promotes neuronal differentiation and plays a crucial role in neuronal maturation and self-renewal [170-172]. ROS, namely, superoxide ($O•^-$), hydrogen peroxide (H_2O_2), and hydroxyl free radicals (HO•) are generated intracellularly as part of normal cellular metabolic byproduct. ROS are mainly produced by membrane-bound NADPH oxidase (NOX) complexes, mitochondria, and endoplasmic reticulum in mammalian cells whose low to moderate levels regulate cellular proliferation, differentiation, and survival [173-175]. However, their excessive and uncontrolled production can result in oxidative stress and damage cellular physiology and functions, often leading to apoptosis and a variety of disorders. Therefore, a balance between ROS generation and scavenging systems is needed to maintain redox homeostasis.

The past findings indicated sub-lethal levels of intracellular ROS could impact cellular signaling cascades in a variety of neuronal and non-neuronal cells by influencing cell proliferation, differentiation and gene expression. ROS has been found to control microbial eukaryotes differentiation process [176], plant's intracellular signaling pathways [177], angiotensin II-mediated renal growth and differentiation [178], and effect differentiation of cardiac stem cells [179]. ROS have been shown to be essential for the NGF-induced differentiation of PC12 cells via TrkA [180], high levels of $O_2•^-$ influence neuronal plasticity and promote neural differentiation in mouse neural stem cells via regulation of PI3K-AKT signaling [181]. Redox state has also been known to modulate differentiation of mesencephalic precursors [182], of neural crest stem cells [183], of oligodendrocyte-type-2 astrocyte progenitor cells progenitors [184] and multipotent adult stem cells [185]. ROS can affect numerous aspects of neural differentiation and function, including the survival and the plasticity of neurons, the proliferation of neural precursors, neuronal maturation, and their differentiation into specific neuronal cell types. Based on several studies reported in the above

literature, it may be hypothesized that ROS generation during stem cell differentiation participates in the dissociation of nuclear factor-erythroid factor 2-related factor 2 (Nrf2) from its repressor protein complex, Kelch-like ECH-associated protein 1 (KEAP1) and cullin-3 (Cul3) into the cytoplasm. This could lead to the activation of neural-specific transcription factors to support lineage-specific differentiation of stem cells.

3.2 Viability and proliferation of hMSCs on metal-doped TiO_2 coated platforms

Tetrazolium reduction assay was performed to estimate the percentage viable cells after 24 h and time-dependent proliferation rate of hMSCs on glass substrate (control) and TiO_2 coated platforms without and with dopants. All the platforms were sterilized with UV light for 15 min before cell seeding. 5 X 10^3 viable cells counted using a manual hemocytometer were seeded on above-described substrates in complete growth media and at 37°C and 5% CO_2 atmosphere. The viability was measured at 24 h, while the cell proliferation was assessed at days 1, 2 and 3 following cell seeding. After a specified period, MTT assay was performed by adding 10 µl of 2 mg/ml MTT solution prepared in PBS and was incubated for 4 h at 370C. Afterward, the supernatant was removed completely from each well, followed by the addition of 100 µl of DMSO to dissolve MTT formazan crystals and further incubated for 30 min. Finally, absorbance was measured at 570 nm using a microplate reader. All the experiments were performed in triplicates. **Figure 3.1** shows cell viability results obtained at different TiO_2 surfaces with and without doping of different transition metal ions. The outcomes were also compared to the control condition described as the glass substrate which was the same on which the coating of TiO_2 by dip coating had been done.

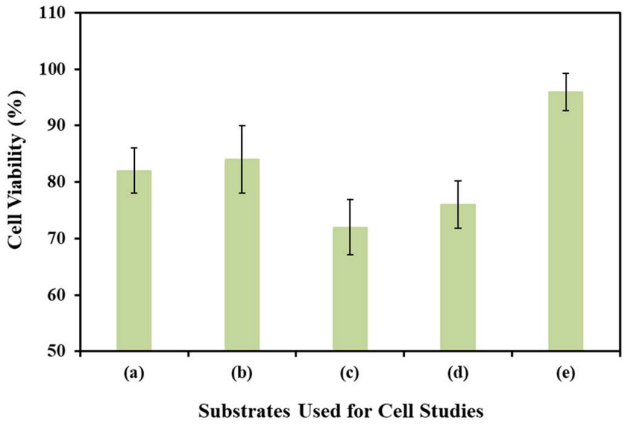

Figure 3.1: Cell viability on (a) control conditions grown on tissue culture plastic surface, (b) TiO_2 thin films coated on the transparent glass surface, and TiO2 doped with (c) Ni, (d) Au and (e) La. ♦ represent <0.5 p significance value for control and doped TiO_2 least response, ♦♦ represent <0.5 p significance value for doped and TiO2 response and ♦ ♦♦ represent <0.5 p significance value for control and doped TiO_2 highest response.

The cell viability was also evaluated using a dual staining fluoresnce method. The populations of viable and dead cells were visualized by Hoechst 33342/PI after 24 h of cell seeding on different substrates. Hoechst 33342 is a cell-permeable dye that stains the DNA of both viable and non-viable cells with blue colour. In contrast, the red fluorescent PI, a cell impermeable dye, stains the cells which are dead. After 24 h of incubation, the media was removed and cells were gently flushed twice with PBS. Afterward, cells-laden platforms were stained with Hoechst 33342 (1 μg mL^{-1}) and PI (1 μg mL^{-1}) solutions and incubated for 30 min at 37°C in the dark. The cells were washed twice with PBS before imaging.

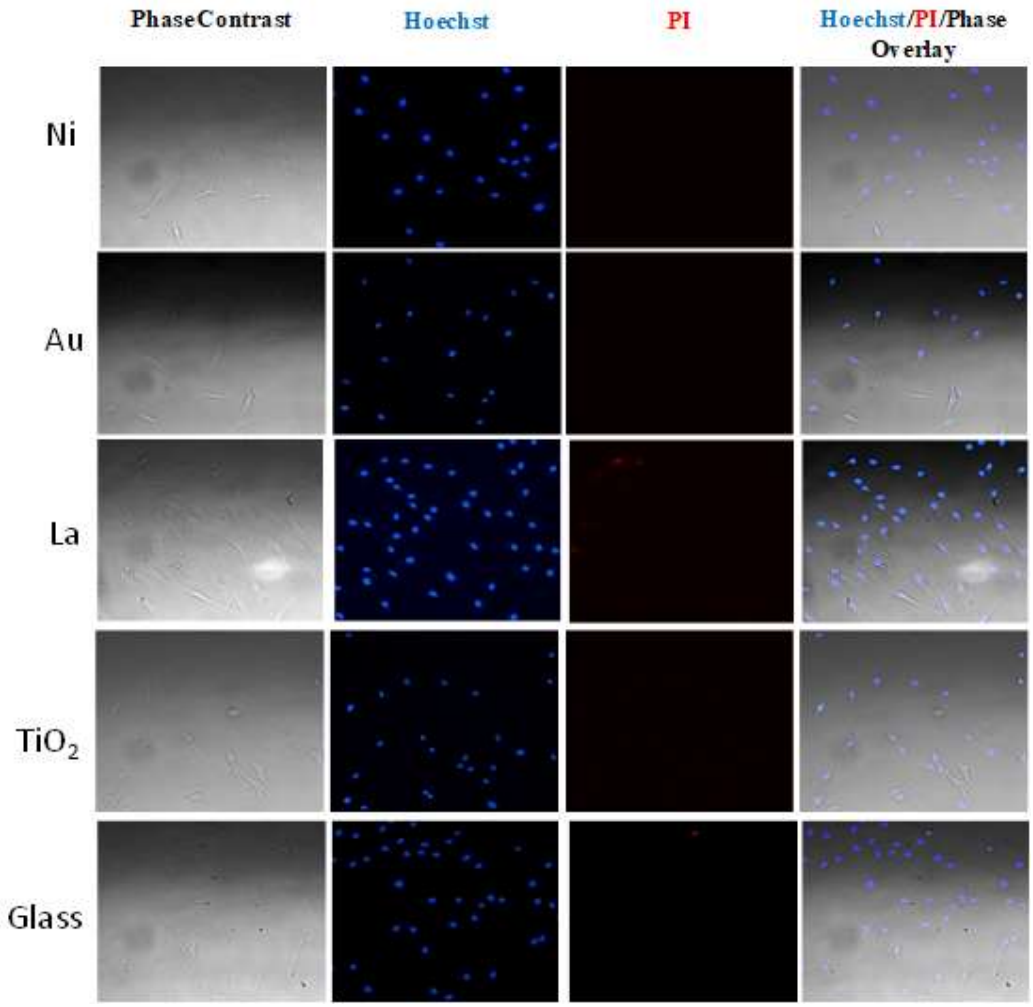

Figure 3.2: Fluorescence Representation of viable vs dead cell populations visualized by staining with Hoechst 33342/PI after 24 h of cell seeding on different substrates. Images are captured at 20 X magnification.

The fluorescence images were captured in phase-contrast mode along with blue and red channels using an inverted fluorescence microscope (Nikon Eclipse 90i) and the results are shown in **Figure 3.2**. The cell viability result concluded from the MTT assay coincides with

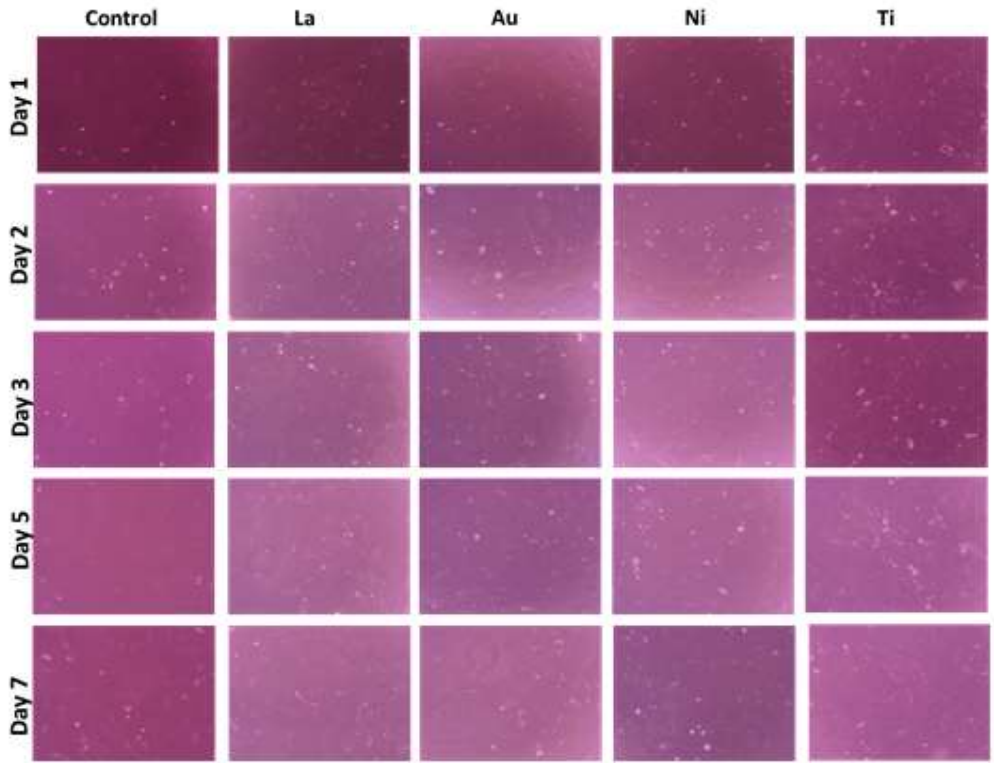

Figure 3.3: Microscopic images of cells captured at different days after cell seeding on different substrates. Ti represents TiO_2 substrate whereas La, Ni and Au representing doping of these metal ions into TiO_2 substrates. Images are captured at 10 X magnification.

the findings of Hoechst 33342/PI dual staining. The fluorescence images did not show any non-viable red population of cells, indicating the biocompatibility of the fabricated platforms for MSCs. The viable cell population was relatively higher for La doped TiO_2 relative to other doped platforms and control condition. The high viability may be attributed that La is having relatively higher atomic radii in comparison to used other transition metal. Thus, it might be playing a role in controlling the surface charge as there was no significant difference in the crystallite structure of TiO_2 as described in the Chapter 2.

Phase contrast microscopic images of cells were captured at different days after cell seeding on different substrates and results are shown in **Figure 3.3**. Relatively an increase in the cell population observed in doped TiO_2 surfaces.

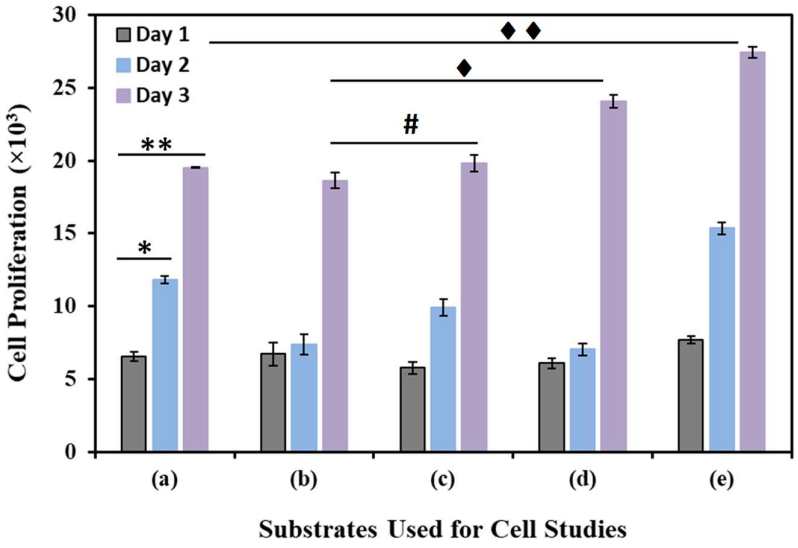

Figure 3.4: Cell viability on (a) control conditions grown on tissue culture plastic surface, (b) TiO_2 thin films coated on the transparent glass surface, and TiO2 doped with (c) Ni, (d) Au and (e) La. ♦ represent <0.5 p significance value for control and doped TiO_2 least response, ♦♦ represent <0.5 p significance value for doped and TiO2 response and ♦ ♦♦ represent <0.5 p significance value for control and doped TiO_2 highest response.

Using MTT assay on also performed to measure the cell proliferation capability. The results of MTT assay are summarized in **Figure 3.4** at day 1, day 2, and day 3 for various substrates. The results showed that the cell growth rate was substantial higher for doped platforms relative to TiO_2 coating and control. Relatively overall an increase in the cell population with time was observed in all doped TiO_2 surfaces at day 3 of cell seeding.

3.3 Neurogenic differentiation of hMSCs on metal-doped TiO_2 coated platforms

To analyze the neural phenotypic plasticity of hMSCs after culturing them on different engineered platforms, the expression of neurogenic markers was validated by immunocytochemistry. We choose to detect three protein markers, namely nestin, β tubulin-III, and GFAP.

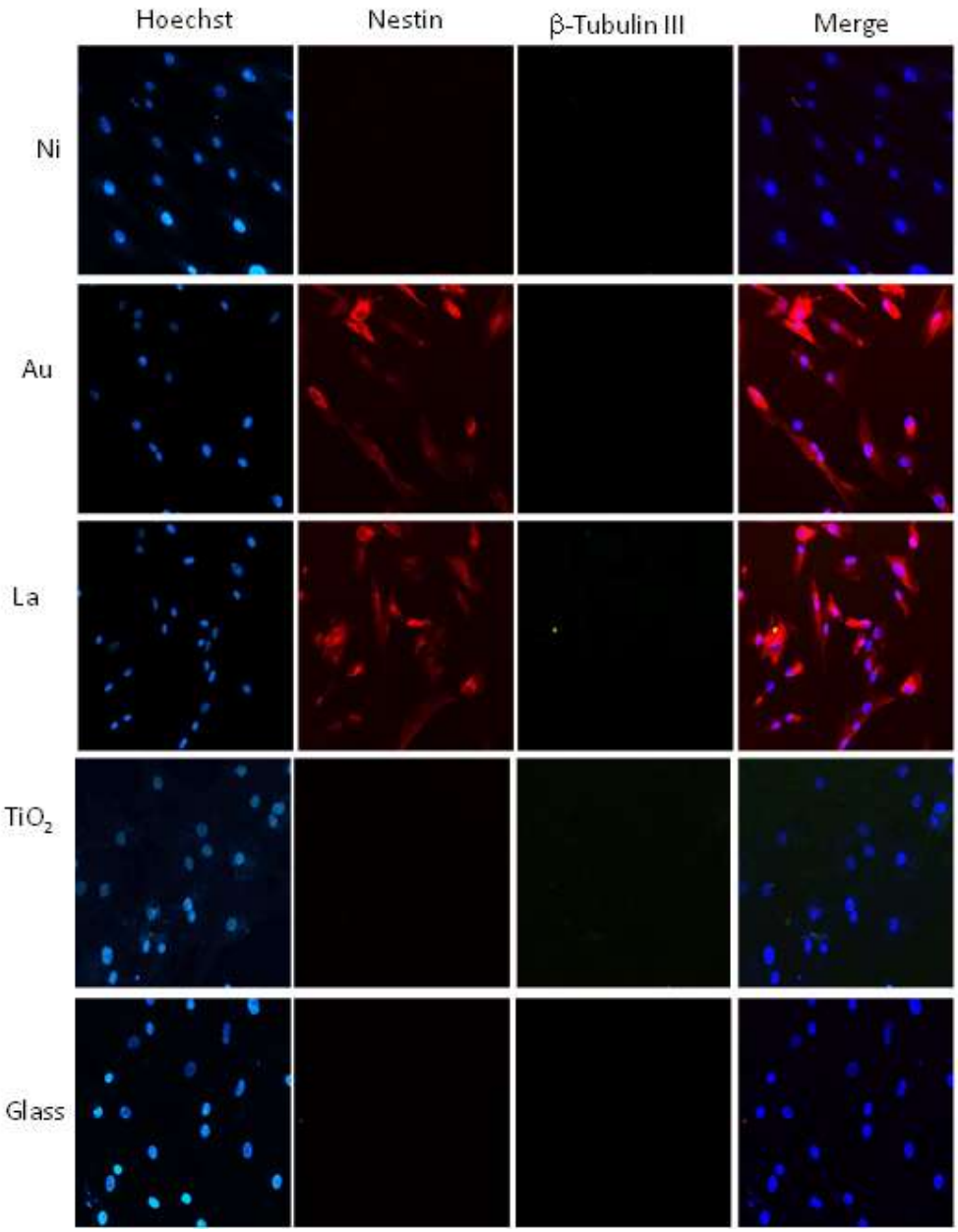

Figure 3.5: Expression of neural-specific markers on different substrates at day 1 of cell seeding. Images were acquired at 20 X magnification.

Figure 3.5, **Figure 3.6** and **Figure 3.7** shows the representative images of hMSCs immunostained across the range of different platforms relative to control for days 1, 3, and 7, respectively. Experiment details are included in annexure I.

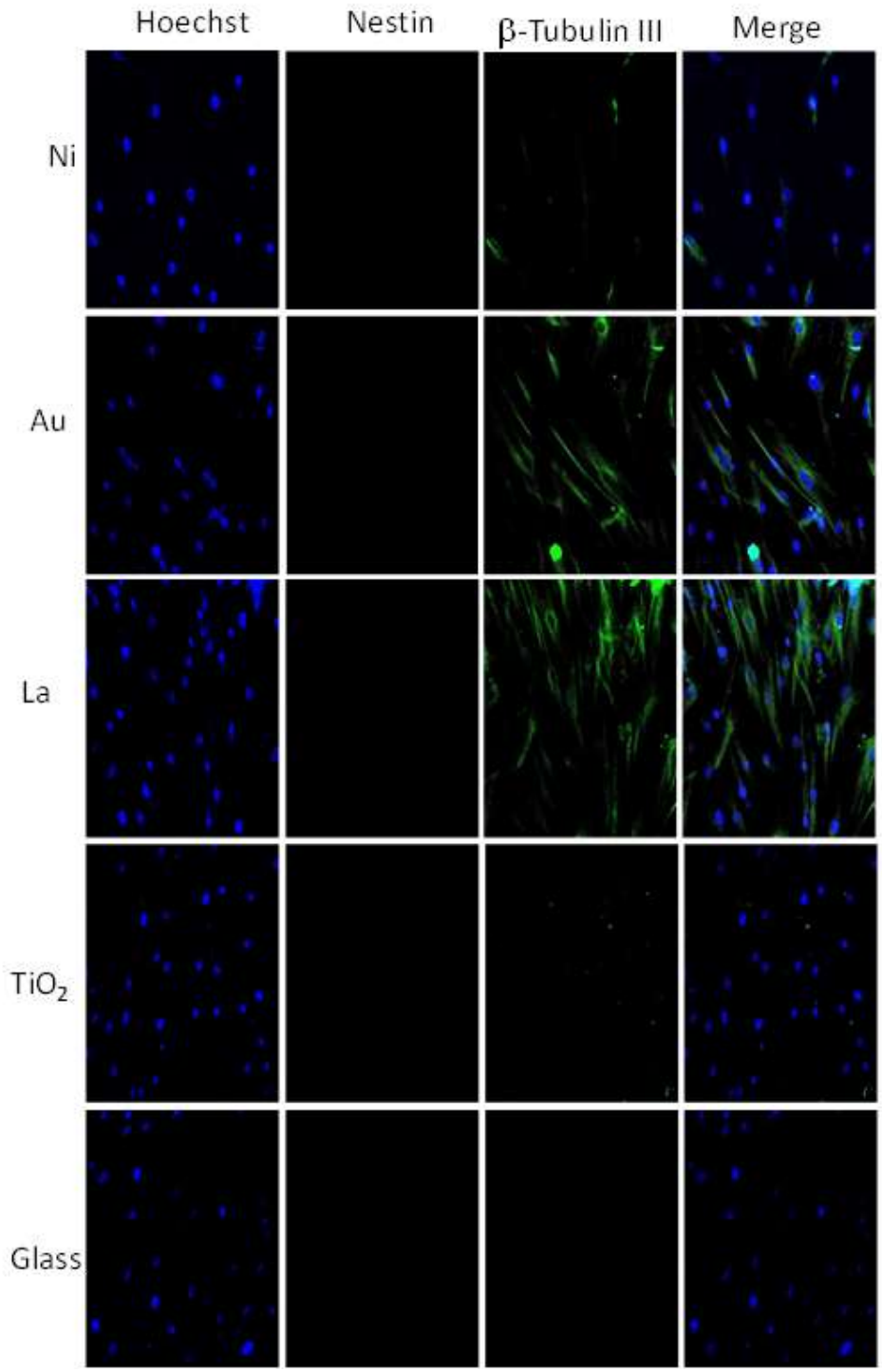

Figure 3.6: Expression of neural-specific markers on different substrates at day 3 of cell seeding. Images were acquired at 20 X magnification.

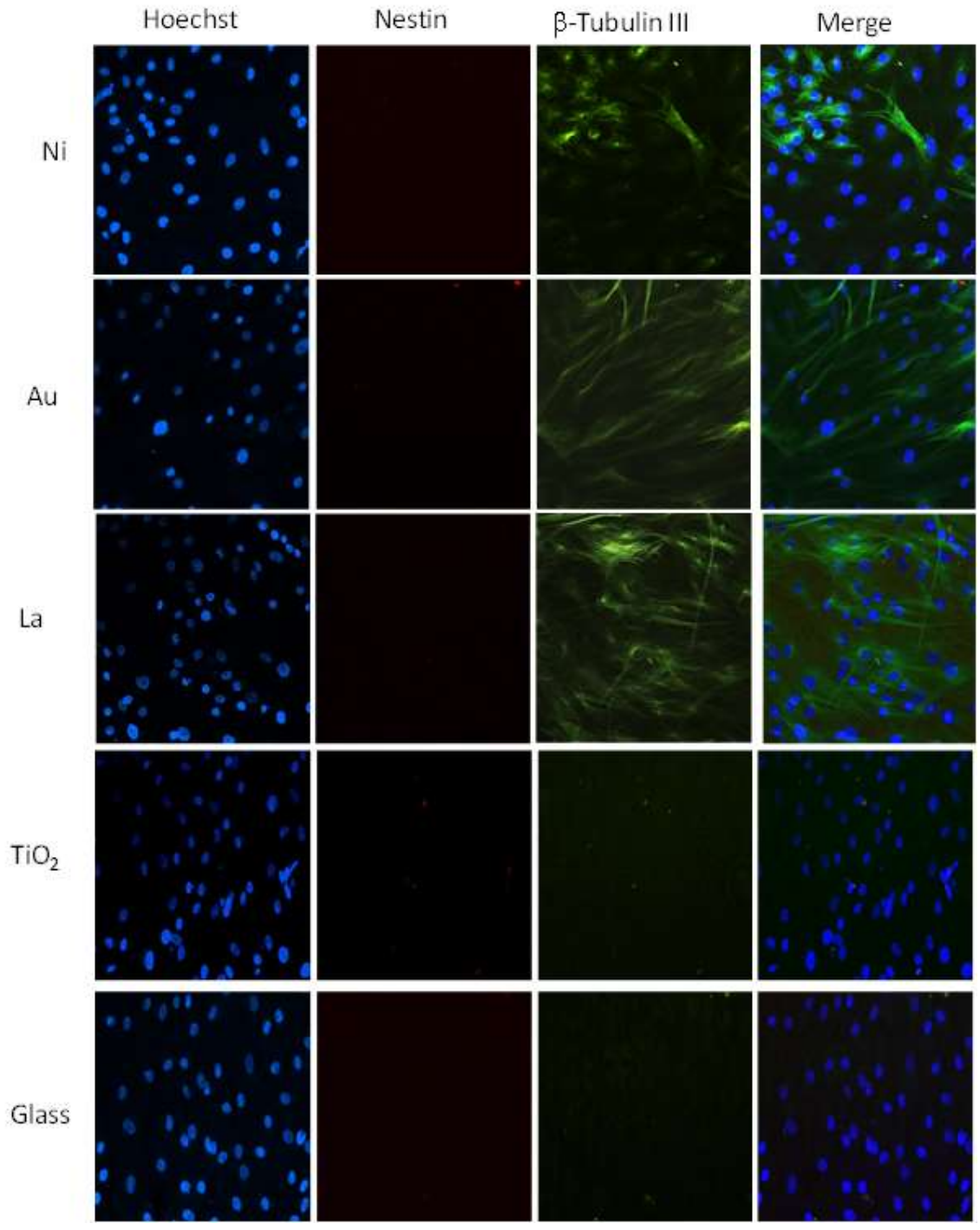

Figure 3.7: Expression of neural-specific markers on different substrates at day 7 of cell seeding. Images were acquired at 20 X magnification.

After 24 h of hMSCs seeding, nestin immunoreactivity was observed for La and Au doped TiO_2, while no expression was detected for other conditions, including control. A notable level of β tubulin-III expression was observed after three days of seeding on La and Au doped TiO_2, as shown in Figure 3b. However, the cells remained negative for β tubulin-III antibody for Ni doped TiO_2, undoped TiO_2 and glass (control). On seventh day, a higher degree of green fluorescence signal was observed for La and Au doped TiO_2 along with Ni doped TiO_2, as represented in Figure 3c. The elongation in cell morphology indicated transition of flat, spindle-shaped hMSCs to enlongated neuronal cells (Figure 3c). However, cell on control and undoped TiO_2 remained unstained for β tubulin-III, as can be realized from the Hoechst labeled nuclear region, that are stained blue without any tinge of green fluorescence. The result indicated that the introduction of dopants in TiO_2 structure induces commitment of hMSCs towards neuronal lineage. However, the process of differentiation is substantial if the dopant has instrinsic characteristics of being a less electronegative element so that if has more tendency of providing its electron to the neighbouring atoms. Among all dopants, La was having minimum electronegativity and with high photocatalytic activity [186]. In chemistry, photocatalysis is the acceleration of a photoreaction in the presence of a catalyst. In catalyzed photolysis, light is absorbed by an adsorbed substrate. In photo-generated catalysis, the photocatalytic activity (PCA) depends on the ability of the catalyst to create electron–hole pairs, which generate free radicals (e.g. hydroxyl radicals: •OH) able to undergo secondary reactions. The expression of nestin is attributed to an early neuronal commitment indicating a population of neural progenitor cells having the tendency to differentiate into glial cells (astrocytes and oligodendrocytes) besides neurons.

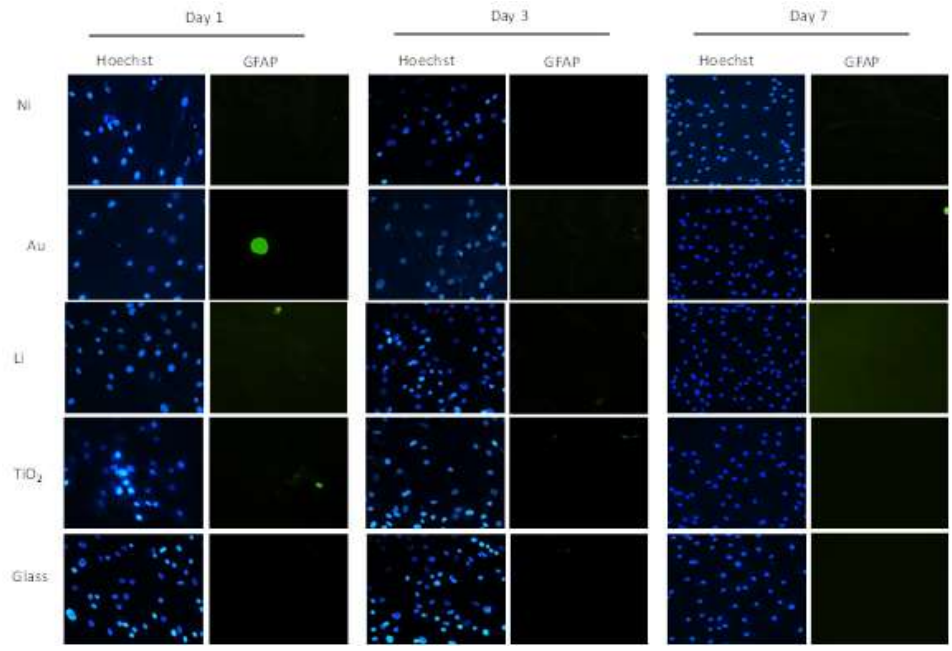

Figure 3.8: Expression of GFAP on different substrates at day 1, day 3, and day 7 of cell seeding. Images were acquired at 20 X magnification.

To evaluate the potential of fabricated platforms for triggering differentiation towards glial cells time-dependent expression of GFAP, expressed by astrocytes, was performed and results are shown in **Figure 3.8**. The fluorescence images taken on different days of cells seeded on different platforms and glass did not express GFAP markers. This indicated the neural progenitor cells are not transforming towards other neural sub-types.

3.4 Quantification of intracellular ROS in Cells seeded on metal-doped TiO_2 coated platforms

To understand the cellular mechanism behind the initiation of neurodifferentiation of hMSCs seeded on doped TiO_2, alteration in intracellular ROS was quantified using a fluorescent dye, DCFH-DA. Earlier studies have found ROS as a key messenger for directing the differentiation process towards neuronal lineage [170-172, 187].

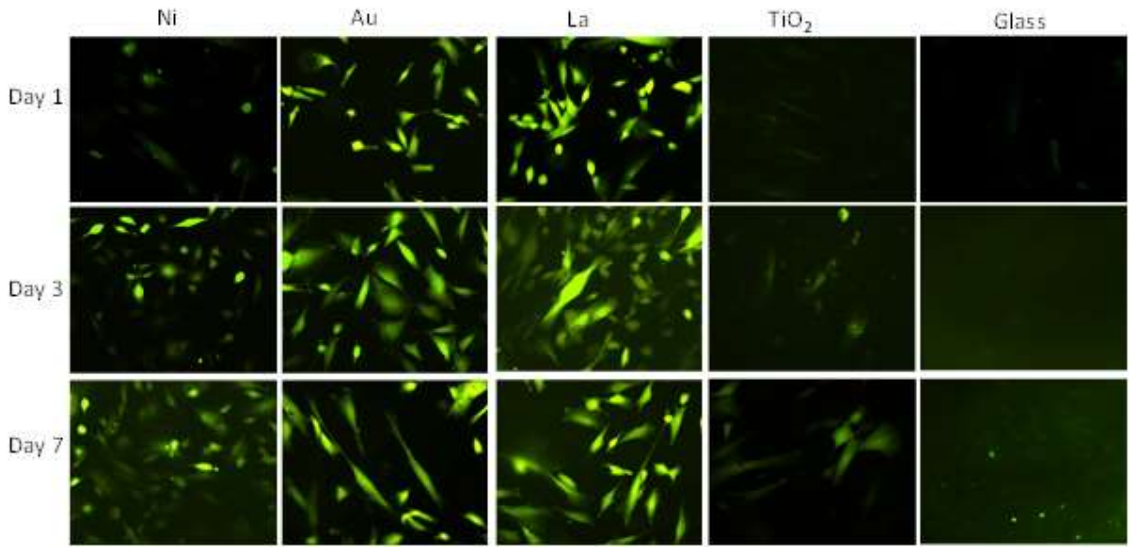

Figure 3.9: Expression of ROS on different substrates at day 1, day 3, and day 7 of cell seeding. Images were acquired at 20 X magnification.

Time-dependent analysis of ROS in cells grown in different conditions showed similar findings as reported earlier. The green fluorescence signal was detected in cells seeded on La and Au doped TiO_2, which elevated as time progressed, indicating ROS-induced neural differentiation of hMSCs, as indicated in **Figure 3.9**. Experiment details are included in annexure I.

The estimation of ROS had been also done through the spectroscopic determination with the use of microplate reader and results are shown in **Figure 3.10**. The details of experimental methodology are given in annexure I. The expression of ROS did not showed significant change in the values for TiO_2 coating on glass, however the doped TiO_2 had significantly influenced the values. The highest expression was observed for La doped TiO_2. The spectroscopic estimation of ROS is consistent with microscopy observation shown in **Figure 3.9**.

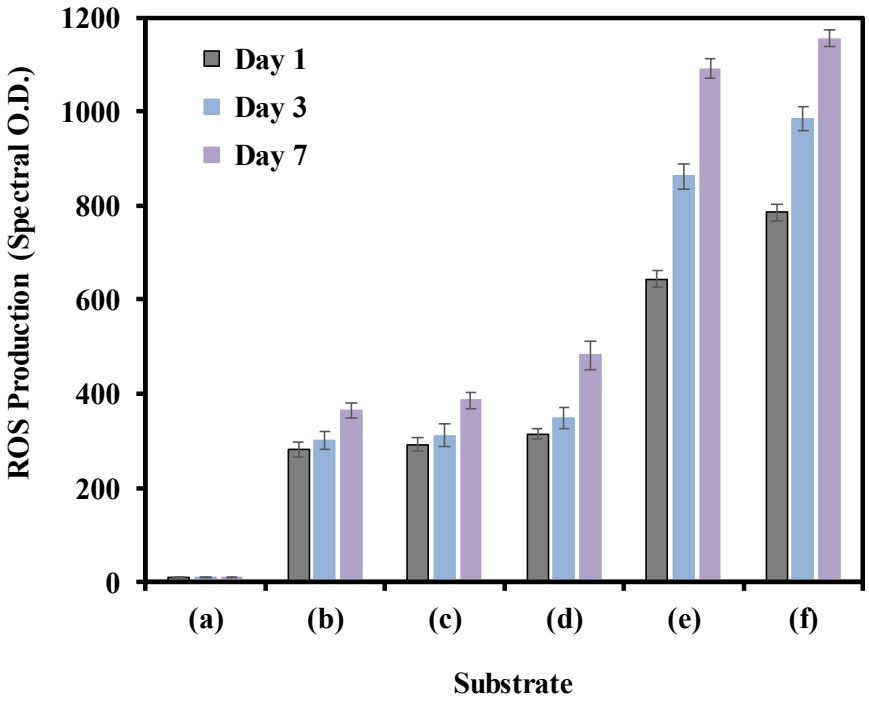

Figure 3.10: Expression of ROS measured by spectroscopic quantification. The plot shows spectral (optical density) corresponds to ROS production on different substrates at day 1, day 3, and day 7 on different substrates for cell number of seeding under similar conditions of the experiment. (a) Blank, (b) glass as a substrate, (c) TiO_2 coated glass as a substrate, (d) Ni doped TiO_2 coated glass as a substrate, (d) Au doped TiO_2 coated glass as a substrate and, (d) La doped TiO_2 coated glass as a substrate.

The result demonstrated La doped TiO_2 platforms supported neurogenic differentiation of hMSCs relatively better than other metal ion dopants. The finding highlighted the role of surface charge in tuning the differentiation process by increasing the level of intracellular ROS, attributing it as an essential secondary messenger for induction of neuro-differentiation.